

## Shaped Charge Jet Initiation of High Explosives equipped with an Explosive Train

Werner Arnold, Markus Graswald

MBDA-TDW Gesellschaft für verteidigungstechnische Wirksysteme mbH, Hagenauer Forst,  
D-86529 Schrobenhausen, Germany

E-mail: [werner.arnold@mbda-systems.de](mailto:werner.arnold@mbda-systems.de), Phone: +49 (0) 8252-99-6267, Fax: +49 (0) 8252-99-6733

### Abstract

In former investigations [1], [2] the initiation behaviour of High Explosives (HEs) when attacked by a Shaped Charge Jet (SCJ) was studied. Two initiation modes: *Impact Initiation* and *Penetration Initiation* were considered while varying between *bare*, *covered* and *cased test set-ups*, depending on the contact between the metal casing and the HE. The results of these trials were applied on real and existing munitions. In the present paper, these continued investigations will be presented.

This time our standard test charge was perforated by the SCJ under different impact angles. Correspondingly, the length of the SCJ crater through the HE varied and simultaneously, the duration of interaction within the HE bulk. Influence on the Explosive Reaction Levels (ERLs) was studied and also the possibility to predict this behaviour with already existing engineering models like Held's  $v^2d$  rule or Jacobs-Roslund's formula.

A second field of investigation will be presented. Our above mentioned standard test charge was additionally equipped with an Explosive Train (ET: booster and detonator with mounting parts). The purpose was to find out if it is possible to initiate or to not initiate (neutralize) the charge with the SCJ via this ET. The corresponding approach was realized by a step-by-step procedure adding more and more parts of the ET while attacking it with the SCJ and measuring the ERLs. Finally, the SCJ perforated the detonator directly under different impact angles and in various locations. The aim was to find out the reaction behaviour of the detonator and its capability to initiate the Booster / HE which is important for applications like C-RAM or the disposal of underwater ship mines.

### 1 Introduction

Figure 1 shows typical test set-ups that were used in previous shaped charge jet (SCJ) initiation trials [1], [2]. We used the more basic investigations (left side) to measure the *run distance to detonation*  $\Delta s$  with the help of a rotating mirror camera for what we called the *bare* (15 mm air gap between steel barrier P and High Explosive (HE)) or the *covered* set-up mode.

The results achieved for the plastic bonded high explosive KS32 (HMX/PB 85/15) are shown in Figure 2. The *jet stimulus*  $v^2d$  ( $v$  = SCJ tip velocity,  $d$  = SCJ diameter) needed to trigger reactions is drastically different for these two initiation modes: *impact mode* (bare charge) and *penetration mode* (covered charge) (see [1], [2]). In-between is the so called *working space* for *cased charges* (Figure 1 right) representative for real munitions.

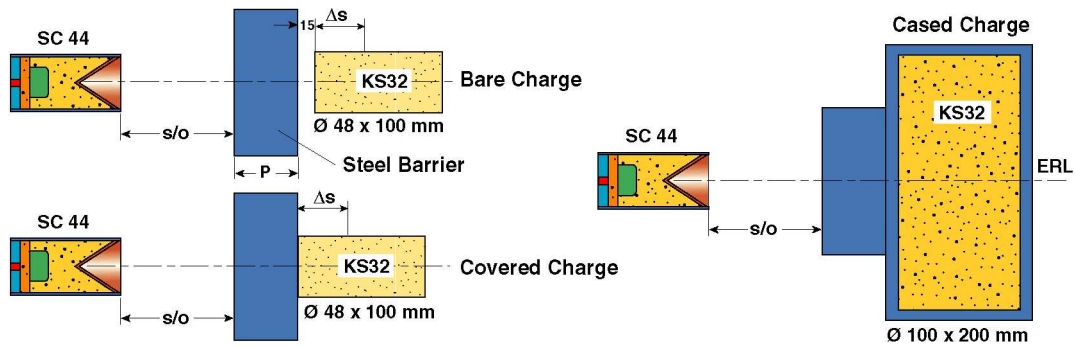


Fig. 1: Three different initiation test set-ups: *bare* and *covered* (left) and *cased* (right).

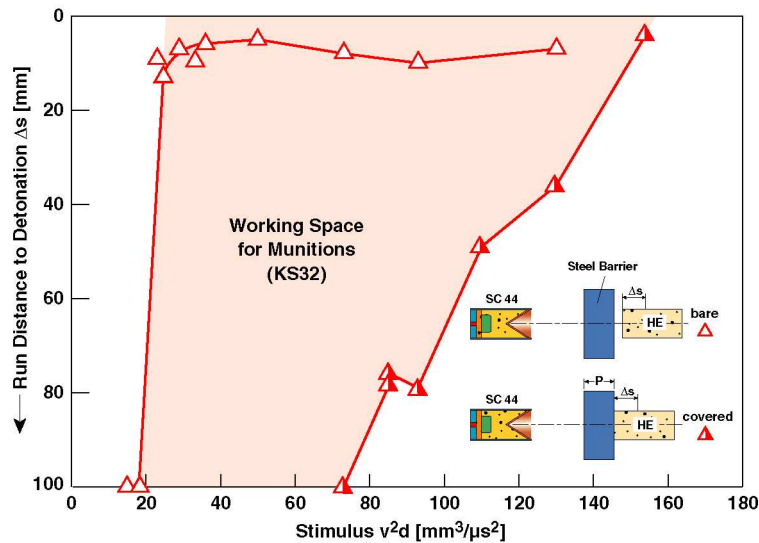


Fig. 2: Sensitivity behaviour of *bare* and *covered* KS32 (HMx/PB 85/15) with the so called *working space* in-between.

## 2 Motivation and Objectives of the Study

For munitions with e.g. air gaps between casing and HE or with voids within the HE the munitions behave similar to a bare charge and the Explosive Reaction Level (ERL) curve would be close to that of a bare charge [1]. That is also true for very thin casings made with low strength materials. On the other hand, if the confinement is very strong as it is for rather thick and/or high strength material casings, the ERL curves for this kind of charges would shift from the covered charge curve into the working space towards the bare charge curve [2].

For the previous studies, the HE length perforated in the different test set-ups was always 100 mm. Two essential questions arise: (Q1) what happens if this length is varied and (Q2) can the behaviour be predicted by formulas like those of Held or Jacobs-Roslund? This was investigated by varying the SCJ impact angle and is discussed in the next section.

A third important aspect - especially for potential applications in underwater ship mine disposal or C-RAM (countering rockets, artillery shells and mortar grenades) – was: can the detonator of an Explosive Train (ET) be activated or neutralized without initiating the whole charge? This topic will be discussed in the fourth section.

### 3 SCJ Initiation Trials with varying Impact Angles

#### 3.1 Test Charge and Set-up

The same test charge dimensions as in [1] were used. Figure 3 shows this standard charge with a HE diameter of  $\varnothing 100$  mm and a length of 200 mm. Two different TDW-HE formulations were tested:

- KS32: HMX/PB 85/15, density  $\rho = 1.65$  g/cc (also used in previous studies)
- KS33: HMX/PB 90/10, density  $\rho = 1.68$  g/cc

The casing consisted of 10 mm mild steel (St35) with only one lid fixed with a thread on the cylindrical section. The respective barriers also consisted of mild steel (C15) with varying thickness  $P$  to adapt the stimulus  $v^2 d$  to the appropriate values.

As indicated in Figure 3, three different impact angles  $\theta$  were applied, leading to three different shot line lengths  $s_{HE}$  through the HE:

- Impact angle  $\theta = 0^\circ$ , shot line length  $s_{HE} = 100$  mm
- Impact angle  $\theta = 30^\circ$ , shot line length  $s_{HE} = 115$  mm
- Impact angle  $\theta = 60^\circ$ , shot line length  $s_{HE} = 200$  mm

A 44 mm calibre Shaped Charge (SC 44) by TDW was used for all test series. A calibration curve: "barrier thickness  $P$  vs. jet stimulus  $v^2 d$ " was available from previous studies and took into account the different lines of sight (LOS) and the 10 mm steel casing. As standoff  $s/o$  always 90 mm ( $\sim 2$  calibres) were used.

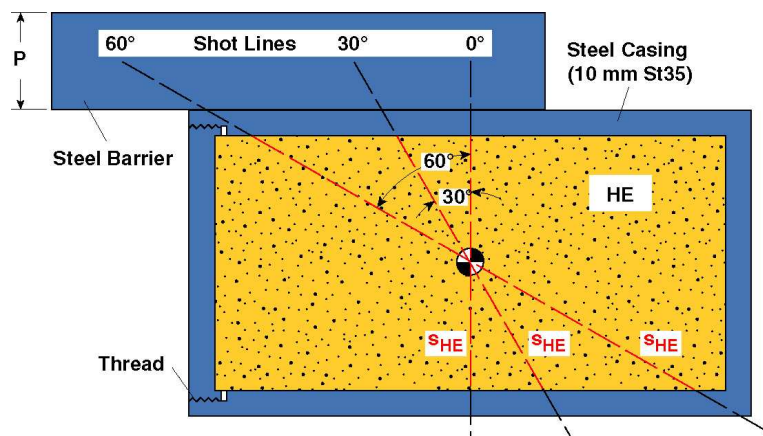


Fig. 3: Standard test charge with steel barrier  $P$  and three different SCJ impact angles  $\theta$ .

For the cased charges, the ERLs were assessed according to MIL-STD 2105C with six different levels. The assessment levels were inferred from the fragment impact pattern obtained on a 4 mm thick mild steel witness panel (1 m x 2 m) in a distance of 2 m from the test charge. Lower level reactions could be determined with the residues of the charge and by the casing disruption. Typical ERL levels achieved during the trials are shown in Figure 4.



Fig. 4: Typical explosive reaction levels (ERL) achieved during the SCJ initiation tests.

### 3.2 Test Prediction with Jacobs-Roslund

In reference [1] the application of the  $v^2d$  rule worked quite well predicting the reaction behaviour of plastic bonded charges. The Jacobs-Roslund (JR) model [3]:

$$v_{crit} = \frac{A}{\sqrt{D_p \cdot \cos \theta}} \cdot (1 + B) \cdot \left( 1 + \frac{C \cdot t}{D_p} \right)$$

is an extension of this  $v^2d$ -rule ( $D_p$  = projectile diameter): this model was mainly developed to describe the initiation behaviour of charges hit by fragments and projectiles. The main question was: does this model also describe the SCJ trial results while varying the impact angle  $\theta$ ? In this case, the necessary stimulus  $v^2d$  (JR nomenclature  $v_{crit}^2 D_p$ ) to achieve a certain ERL would have to rise when the impact angle  $\theta$  increases.

### 3.3 Test Results for KS32 & KS33

Several test charges were assembled for each HE formulation and for each angle variation series. The ERLs were assessed against the SCJ stimulus  $v^2d$  as described above and were entered into a diagram as a summary for each HE formulation. The results for KS32 are shown in Figure 5 and for KS33 in Figure 6 respectively.

#### **KS32 (HMX/PB 85/15), Figure 5**

The behaviour of KS32 under  $0^\circ$  impact angle was already known from [1]. There is a relatively smooth increase in the reactivity of this plastic bonded HE while increasing the stimulus. Contrary to the expectation - when applying JR's model - the stimulus necessary to achieve a certain ERL decreased while the impact angle increased. Or in other words: under the same stimulus, reactivity of KS32 is the higher the larger the impact angle is. This means the JR model doesn't describe the SCJ initiation behaviour correctly with regard to the impact angle. It is obvious that the length of the perforated HE is the significant parameter which determines the reaction level. The longer the SCJ path through the HE, the more time is available for interaction and especially for building up higher reactivity levels. The behaviour seems to be non-linear: the three curves are roughly equidistant while the shot line length  $s_{HE}$  increase is rather different for the three impact angles.

#### **KS33 (HMX/PB 90/10), Figure 6**

The situation for KS33 is comparable to that of KS32 with regard to the varying impact angle. Also here the JR model is not valid and cannot be applied. But there are also significant differences between these two formulations. For normal SCJ impacts ( $0^\circ$  impact angle) the KS33

behaviour is rather “digital” i.e. the transition between *no reaction* (ERL ~ VI) and *reaction* (ERL ~ I) is abrupt (a step function) within a very small stimulus range. For the 30° impact the transition appears to be somewhat smoother. This behaviour can’t be explained at the moment. For the 60° series the stimulus value for the reactivity transition seems to be smaller than it is the case for KS32. Unfortunately there were not enough test samples available in time to exactly determine this transition value.

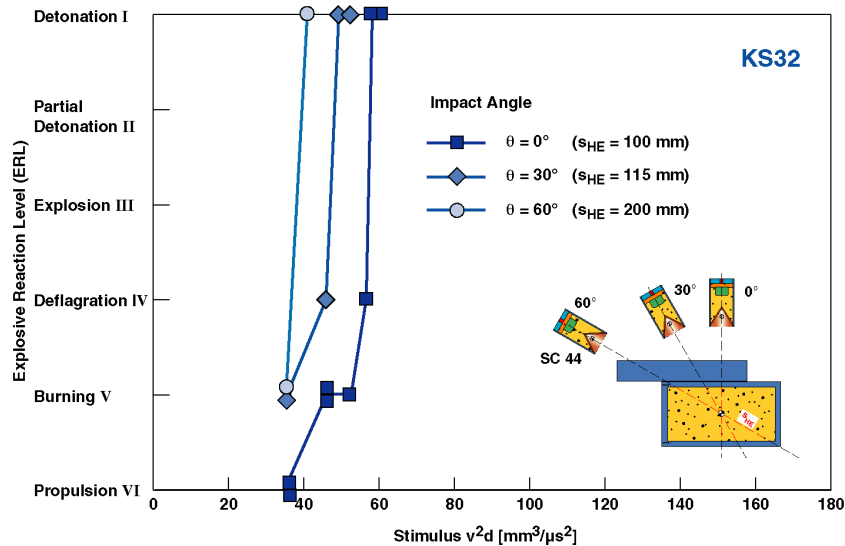


Fig. 5: Summary of results for KS32 (HMX/PB 85/15).

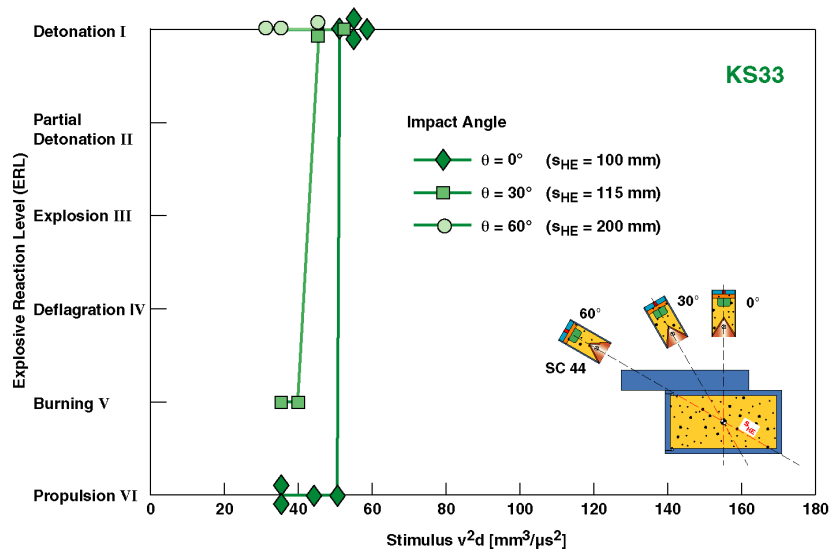


Fig. 6: Summary of results for KS33 (HMX/PB 90/10).

### 3.4 Conclusion 1: Impact Angles

SCJ firings were carried out under varying impact angles against our standard charge filled with two different TDW PBXs: KS32 (HMX/PB 85/15) and KS33 (HMX/PB 90/10). The reactivity of both HEs increased with increasing shot line length  $s_{HE}$  due to the longer interaction time. The Jacobs-Roslund formula cannot predict this behaviour correctly. Therefore, the geometry of the charge (length of perforated HE) has to be also taken into account in a future improved initiation model for SCJ impacts.

Additionally KS33 showed (at least under 0° impact angle) a more step-like reaction behaviour compared to KS32. An explanation for this effect can’t be given at the moment.

## 4 SCJ Initiation Trials on Charges equipped with an Explosive Train

### 4.1 Test Charge and Set-up

The test charge was mainly the same as in the previous section: again, a 10 mm mild steel (St35) casing with just one lid fixed with a thread was applied. This time, the HEs used for main charge and booster charge each were (reasons see below):

- KS22a (main charge): RDX/Al/PB 67/18/15, density  $\rho = 1.65 \text{ g/cc}$ ,  $p_D \sim 47 \text{ kbar}$
- HNS (booster charge): HNS/Wax 95/5, density  $\rho = 1.60 \text{ g/cc}$ ,  $p_D \sim 37 \text{ kbar}$

with  $p_D$  as pressure where a detonation starts – measured by the TDW gap test ( $\sim 20 \text{ mm}$  run distance  $\Delta s$ ).

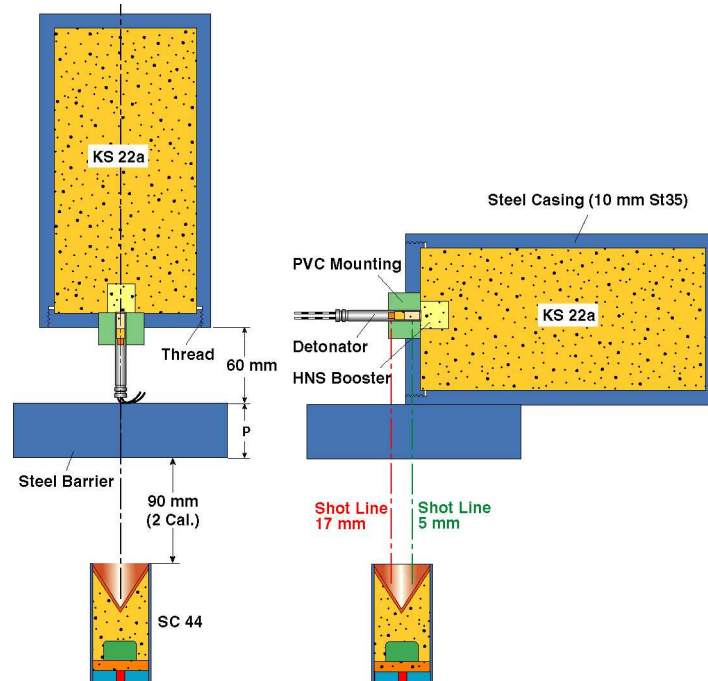


Fig. 7: Test set-ups for the explosive train (ET) initiation trials: axial variant (left) and radial variant (right).

The essential difference to the standard test charge is the additional generic explosive train (ET, see Figure 7) comprising the HNS booster (Hexanitrostilben) with a diameter of  $\text{\O}12 \text{ mm}$  and a length of  $18 \text{ mm}$  and a detonator (No. 8) with dimensions and primary / secondary HE loadings as shown in Figure 8. This detonator was mounted to the steel casing with a plastic (PVC) cylinder ( $\text{\O}30 \text{ mm} \times 20 \text{ mm}$ ) with a bore hole big enough to fit the detonator body in. We selected the detonator No. 8 for two reasons: firstly, as a typical test range detonator it was available; secondly - and even more important - because of the big amount of secondary high explosive loading ( $650 \text{ mg PETN}$ ). The idea behind this was: if we succeed in neutralizing this powerful detonator by a SCJ without initiating the booster / main charge then it should be also possible – and even easier - to neutralize less powerful ones.

Concerning a real existing munition, the fuze / ET parts cannot be shot at by a SCJ under any arbitrary angles. This certainly would depend on a case-to-case decision. Therefore we decided to select the two most extreme situations for our standard generic charge: *axial* and *radial shot lines* as already indicated in the sketches for the test set-ups shown in Figure 7.

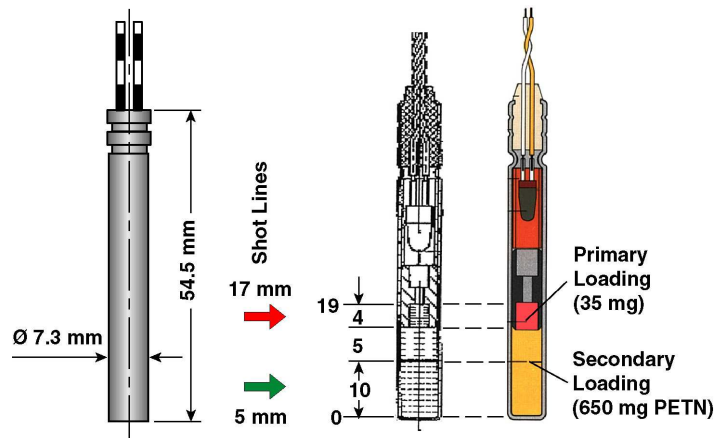


Fig. 8: Detonator No. 8: dimensions and primary / secondary HE loadings. The (red / green) arrows indicate the radial shot line directions during the trials.

#### **Axial test variant (Figure 7 left)**

The  $v^2d$  value of the SC 44 jet is again tuned with a mild steel (C15) barrier with variable thickness P. This jet perforates the ET with detonator and booster and finally enters the main charge. Now when a high level reaction occurs it is not clear where it started and which part of the charge is responsible for it. Therefore a stepwise procedure with different variants of the test charge was necessary - as explained in the next section. The sensitivities S of the different high explosives involved are decreasing along the shot line:

$$S(\text{primary}) > S(\text{secondary}) > S(\text{HNS booster}) > S(\text{KS22a main charge})$$

#### **Radial test variant (Figure 7 right)**

Two SCJ shot lines are interesting (see Figure 7 right and Figure 8):

- through the primary loading of the detonator (17 mm from the bottom of the detonator: red arrow) and
- through the secondary loading of the detonator (5 mm from the bottom of the detonator: green arrow)

The steel barrier P tailors the  $v^2d$  value while with the 5 mm shot line (green) also the thickness of the casing and of the steel lid (through the centre) is taken into account.

## **4.2 Stepwise Procedure for the Axial Test Variant**

As already mentioned, especially for the axial test variant it is important to know where a reaction starts when the jet perforates the test sample. To localize this starting point, additional three derivatives of the standard charge were designed for the axial test case (see Figure 9):

- Test charge without ET (Fig. 9 left)
- Test charge with integrated HNS booster (Fig. 9 centre)
- Tests charge with booster and PVC mounting cylinder ( $\varnothing 30\text{mm} \times 20\text{mm}$ , Fig. 9 right)

#### **Stepwise Procedure**

First: all of the three charge derivatives were shot at axially with tuned SC 44 jets to find out the reaction transition between low (ERL~ VI) and high reaction levels (ERL~ I). Finally, all the transition curves were drawn into the same graph as a baseline for the axial ET initiation tests. The test series was started with the "blank charge" without any ET part. We shot at this charge both, axially and radially to check the hypothesis - presented in section 3 - also for a KS22a charge formulation and once more, the axial version with a shot line length of  $s_{\text{HE}} = 200 \text{ mm}$  showed a higher reactivity than the radial version with  $s_{\text{HE}} = 100 \text{ mm}$  (see also Figure 11 or 12).

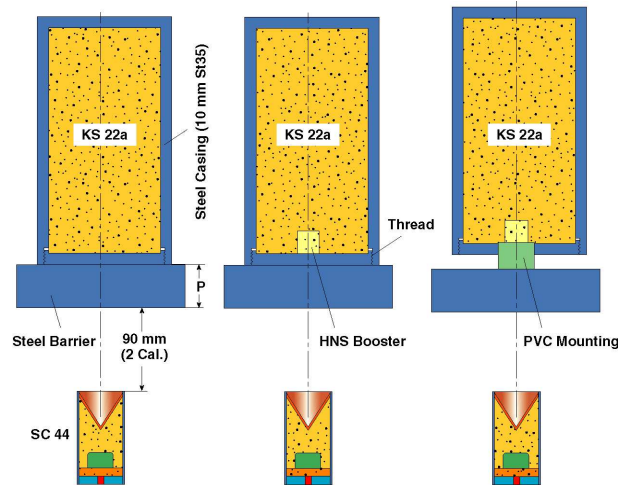


Fig. 9: Three additional test derivatives of the standard charge for the stepwise test procedure

Second: as expected, the charge derivative with the “HNS booster only” was more sensitive than the blank KS22a due to the lower initiation threshold of HNS. Exemplary for such a transition curve, the test results are shown in Figure 10. The purple reference curve (circles) is from the radial tests with the blank charge while the red curve (triangles) shows the results with the “booster charge”. The insets document the reaction behaviour: at low reaction levels residues of the casing and the KS22a charge can be found while at high reaction levels, the witness panel with holes caused by the natural fragments is used for the assessment. For reference reasons (concerning the witness panels) also a charge was initiated by firing the detonator of the ET.

Third: the transition curve for the test derivative with “booster and plastic mounting cylinder” was further shifted to lower stimuli (higher sensitivities) as it behaves more like a *bare charge* than a *covered charge* (see section 1 and [1]).

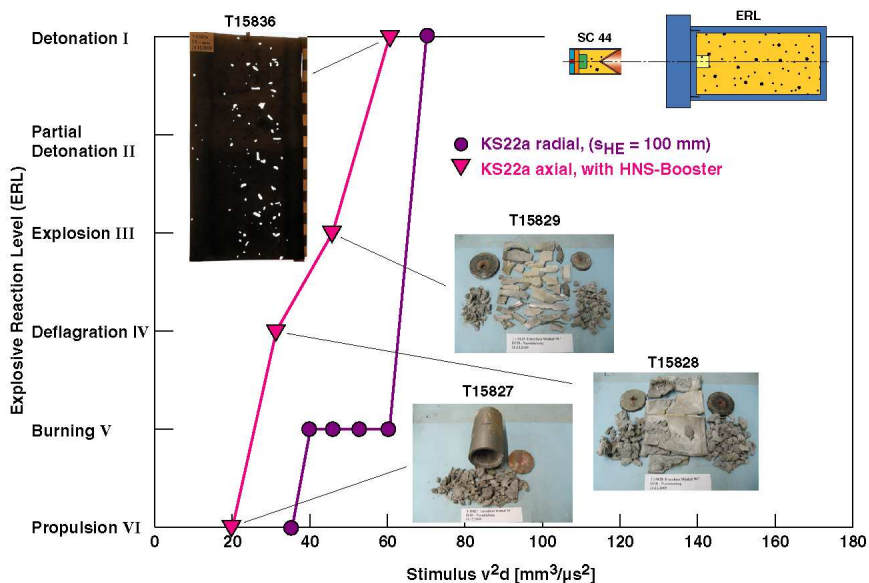


Fig. 10: Examples for the low / high level reaction transition curves of the HNS boosted charge (red triangles) compared with the radially shot reference KS22a charge (purple circles).



### 4.3 Test Results for Axial & Radial SCJ Impact

After carrying out all of these pre-tests with the standard charge derivatives, trials with the ET charges were started beginning with the axial variant and continuing with the radial one.

#### Axial Impact Tests

According to the test set-up of Figure 7, the stimulus  $v^2d$  was chosen small enough to be sure that any initiation of the charge at all could be caused by the primary / secondary HE charge of the detonator No. 8 only. Two shots with rather low stimuli were carried out with the results shown in Figure 11. The graph also includes all curves of the pre-test campaign of the previous section – drawn in grey colour. Those curves are shifted more and more to lower stimuli (left side) due to the increasing sensitivities of the HEs (or longer path  $s_{HE}$  through HE) involved.

Both tests with the ET (shot direction into the detonator as indicated in Figure 11) showed a clear detonation caused by the primary / secondary HE charge of the detonator.

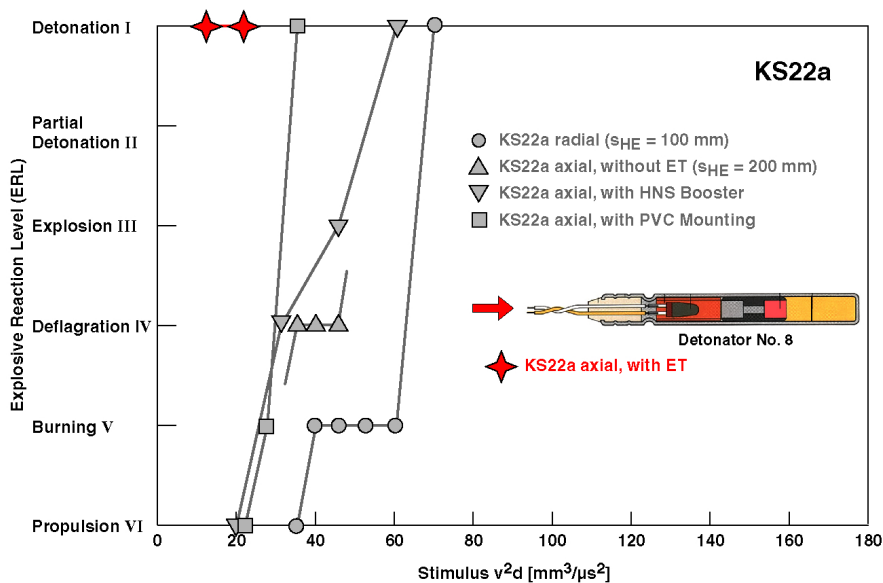


Fig. 11: Results of the pre-test campaign (grey curves) compared with the two axial tests with an explosive train (stars).

#### Radial Impact Tests

Here we have to distinguish between two shot lines:

- 17 mm from detonator bottom: through primary HE loading (red star)
- 5 mm from detonator bottom: through secondary HE loading (green stars)

The results are graphically summarized in Figure 12, again together with the results of the axial pre-test campaign (grey curves). The SCJ shot through the primary detonator loading with a low stimulus showed a clear detonation (red star). The SCJ shot through the secondary detonator loading with a very low stimulus resulted in no reaction at all (green star). A further SCJ shot with a higher stimulus – the same as applied to the primary charge loading (17 mm shot line) - produced exactly the same result: no reaction at all.

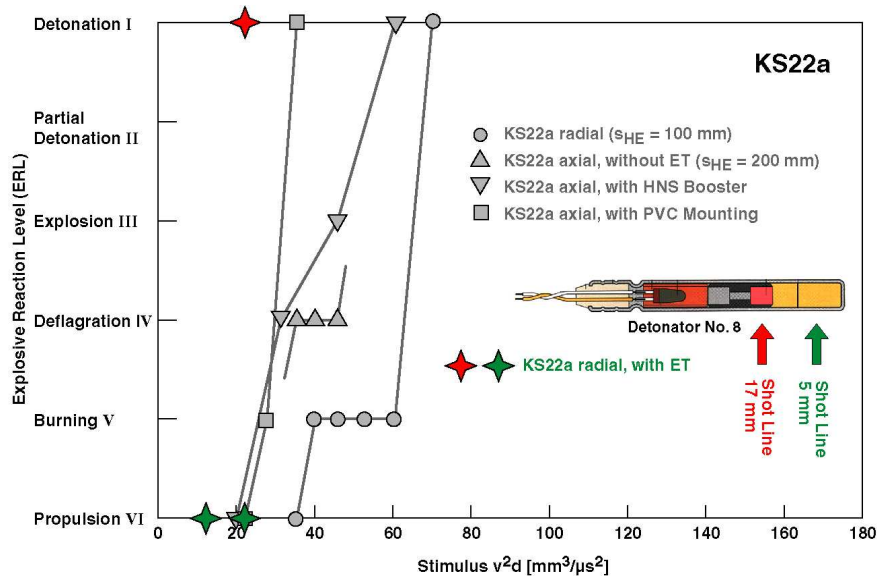


Fig. 12: Results of the pre-test campaign (grey curves) compared with the three radial tests with an explosive train (stars).

#### 4.4 Conclusion 2: Explosive Train

Trials with our standard charge equipped with a generic explosive train (ET) were carried out. As main charge, KS22a and for the booster, HNS were used. Besides this booster, the explosive train also comprised the detonator No. 8 with a primary and a secondary HE loading. Two test set-up versions were used: one axial and one radial variant. In both, the charges were attacked by the SC 44 jet with varying stimulus. For the axial variant, a stepwise procedure with different charge derivatives was necessary. Depending under what impact conditions the detonator of the ET is hit by the SC jet, the main charge detonates or shows no reaction at all.

Thus, the test campaign demonstrated clearly the possibility to neutralize a charge by its explosive train via the secondary HE loading of a detonator. Potential applications are: C-RAM or the disposal of underwater ship mines.

#### Acknowledgement

The authors would like to thank the BWB Team K 6.3 at Koblenz for the funding of this study.

#### References

- [1] W. Arnold, E. Rottenkolber  
*"Sensitivity of High Explosives against Shaped Charge Jets"*  
 2007 Insensitive Munitions & Energetic Materials Technology Symposium (IMEMTS)  
 Miami, FL USA, October 15-18, 2007
- [2] W. Arnold  
*"High Explosive Initiation by High Velocity Projectile Impact"*  
 11<sup>th</sup> Hypervelocity Impact Symposium, Freiburg, Germany, April 11-15, 2010
- [3] L.A. Roslund, J.M. Watt, N.L. Coleburn  
*"Initiation of Warhead Explosives by the Impact of Controlled Fragments in Normal Impact"*  
 NOLTR 73-124, 1975